NanoImpact 29 (2023) 100448

Contents lists available at ScienceDirect

NanoImpact

journal homepage: www.elsevier.com/locate/nanoimpact

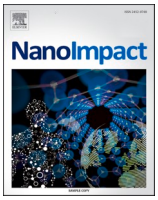

Assessment of skin sensitization properties of few-layer graphene and graphene oxide through the Local Lymph Node Assay (OECD TG 442B)

Silvio Sosa [a], Aurelia Tubaro [a], Michela Carlin [a], Cristina Ponti [a], Ester Vázquez [b,c], Maurizio Prato [d,e,f], Marco Pelin [a,*]

[a] Department of Life Sciences, University of Trieste, Via Fleming 22, 34127 Trieste, Italy
[b] Regional Institute of Applied Scientific Research (IRICA), University of Castilla-La Mancha (UCLM), 13071 Ciudad Real, Spain
[c] Department of Organic Chemistry, Faculty of Science and Chemistry Technologies, University of Castilla-La Mancha (UCLM), 13071 Ciudad Real, Spain
[d] Department of Chemical and Pharmaceutical Sciences, Via Giorgeri 1, University of Trieste, 34127 Trieste, Italy
[e] Center for Cooperative Research in Biomaterials (CIC biomaGUNE), Basque Research and Technology Alliance (BRTA), Paseo de Miramon 182, 20014 Donostia San Sebastián, Spain
[f] Basque Foundation for Science (IKERBASQUE), Plaza Euskadi 5, 48013 Bilbao, Spain

ARTICLE INFO

Editor: Bernd Nowack

Keywords:
Graphene
Skin
Toxicity
Dermal exposure
Hazard characterization

ABSTRACT

Skin contact is one of the most common exposure routes to graphene-based materials (GBMs) during their small-scale and industrial production or their use in technological applications. Nevertheless, toxic effects in humans by cutaneous exposure to GBMs remain largely unexplored, despite skin contact to other related materials has been associated with adverse effects. Hence, this *in vivo* study was carried out to evaluate the cutaneous effects of two GBMs, focusing on skin sensitization as a possible adverse outcome.

Skin sensitization by few-layer graphene (FLG) and graphene oxide (GO) was evaluated following the Organization for Economic Cooperation and Development (OECD) guideline 442B (Local Lymph Node Assay; LLNA) measuring the proliferation of auricular lymph node cells during the induction phase of skin sensitization. Groups of four female CBA/JN mice (8–12 weeks) were daily exposed to FLG or GO through the dorsal skin of each ear (0.4–40 mg/mL, equal to 0.01–1.00 mg/ear) for 3 consecutive days, and proliferation of auricular lymph node cells was evaluated 3 days after the last treatment. During this period, no clinical signs of toxicity and no alterations in body weight and food or water consumptions were observed. In addition, no ear erythema or edema were recorded as signs of irritation or inflammation. Bromo-deoxyuridine (BrdU) incorporation in proliferating lymphocytes from ear lymph nodes (stimulation indexes <1.6) and the histological analysis of ear tissues excluded sensitizing or irritant properties of these materials, while myeloperoxidase activity in ear biopsies confirmed no inflammatory cells infiltrate. On the whole, this study indicates the absence of sensitization and irritant potential of FLG and GO.

1. Introduction

The growing industrial and commercial production of manufactured nanomaterials has been leading to an increased risk for human health by the potential exposure to these materials. In this view, a perfect example is represented by graphene-based materials (GBMs), a family of bidimensional (2D) materials (Geim and Novoselov, 2007), including few-layer graphene (FLG) and its oxidative product graphene oxide (GO), graphene nanoplatelets (GNP) and other functionalized graphene materials (Wick et al., 2014; Bianco et al., 2013). GBMs have been surrounded by increasing interest and expectation due to their unique physicochemical properties. Indeed, basing on their high surface area, extraordinary electrical and thermal conductivity and strong mechanical strength, GBMs are promising tools for a wide range of applications in the fields of nanoelectronics and energy technology, biosensoristic and biomedicine (Guo and Mei, 2014). Given these properties, an active field of research is related to GBM applications at the skin level, mainly as artificial and electronic skin, wound healing materials and smart electronic devices for health-care monitoring directly in contact with the skin (Kim et al., 2016; Shin et al., 2016). For instance, GBMs are the most used nanomaterials for the production of transparent conformable electronic skins (*E*-skins) (Ho et al., 2016), but also for multifunctional

* Corresponding author.
E-mail address: mpelin@units.it (M. Pelin).

https://doi.org/10.1016/j.impact.2022.100448
Received 25 August 2022; Received in revised form 25 November 2022; Accepted 16 December 2022
Available online 21 December 2022

wearable e-textiles materials, equipped with durability, washability and flexibility (Karim et al., 2017). GBMs represent also excellent candidates for the development of 3D scaffolds for tissue engineering, including the skin, mimicking the extracellular matrix (ECM) as structural support in the regenerating tissues, promoting cells growth, angiogenesis and ECM components deposition (Geetha Bai et al., 2019; Thompson et al., 2015).

Thus, at least considering these promising applications, skin contact can be assumed as one of the most important exposure routes to GBMs. However, since the majority of these applications are still at the experimental stage (Park et al., 2017), the risk for human health associated with GBM skin exposure is currently related mainly to the occupational exposure rather than to exposure by consumers. Anyway, skin contact, together with inhalation, may be considered the main exposure route to GBMs during their industrial or laboratory production (Fadeel et al., 2018; Pelin et al., 2018a).

However, epidemiological and clinical data on GBM skin toxicity are currently missing, probably due to the relatively novel and still limited commercialized technology. Only few cases have been reported for related carbon-based materials, such as carbon fibers, able to induce irritant contact dermatitis, as shown in a worker while drilling, cutting and grinding these fibers (Eedy, 1996). Similarly, an epidemiological study involving 746 graphite workers highlighted an increased incidence of skin diseases, such as hyperkeratosis and naevi (Kasparov et al., 1989). Anyway, given the chemical nature of GBMs, the most feasible outcome after cutaneous exposure can be represented by contact dermatitis, which can be either irritant or allergic contact dermatitis, the latter based on skin sensitization. In this view, in the attempt to investigate the skin irritation potential of GBMs, we have recently applied the Organization for Economic Cooperation and Development (OECD) test guideline (TG) 439 as an *in vitro* test, replacing the Draize *in vivo* one, validated also for regulatory purposed. The study used the Reconstructed Human Epidermis (RHE), a fully differentiated three-dimensional epidermal tissue constituted of normal keratinocytes, on which we demonstrated that GBMs with very low residues of surfactants (or GBMs exfoliated with non-toxic agents) are not skin irritants. The study suggested that any irritation potential of these GBMs could derive from surfactant residues in the final product rather than to the graphene material itself (Fusco et al., 2020a).

Even though skin irritation potential of GBMs appeared to be low, skin sensitization cannot be excluded, also considering GBM ability to interact with proteins (Kenry and Lim, 2016; Mondal et al., 2016) with a possible action as haptens to elicit an immune response. In fact, it has been reported that nanomaterials can be detectable by the skin immune system components after their reaction with proteins, such as complement factors and/or damage- and stress-signal proteins produced by cells interacting with the materials (Kotagiri and Kim, 2014). In line with these observations, an *in vivo* study suggested a cell-mediated immune response elicited by exposure to GO. The study used a minimally invasive model to investigate the local immune reaction induced by intradermal GO injection in the growing feather sites of chicks. Results suggested an interaction of this material with host proteins, but no other signs of toxicity (Erf et al., 2017).

Hence, this study was carried out with the aim to investigate the *in vivo* skin sensitization potential of FLG and GO, as representative GBMs, following the specific OECD TG 442B, namely the Local Lymph Node Assay: BrdU-ELISA (OECD, 2018).

2. Materials and methods

2.1. Materials

All reagents of analytical grade, if not otherwise stated, were purchased from Sigma-Aldrich (Milan, Italy). GO (batch #GOB067) was kindly supplied by Graphenea (San Sebastián, Spain). FLG was obtained by ball-milling under solvent-free conditions, as previously reported (León et al., 2011, 2014, 2016). Briefly, a mixture of 7.5 mg of graphite and 22.5 mg of melamine (1,3,5-Triazine-2,4,6-triamine) was ball-milled at 100 rpm for 30 min through a Retsch PM 100 planetary mill under air atmosphere and subsequently sonicated for 1 min in 20 mL of water. Melamine was afterwards eliminated by dialysis and the resulting FLG water dispersion was lyophilized.

Both materials were previously physico-chemically characterized as reported in Table 1. For the complete characterization, refer to our previous studies performed with the same batches of both materials (Fusco et al., 2020a; Cavion et al., 2020).

2.2. Animals

Female CBA/JN mice (18–20 g body weight, 10-week old), bedding and feed were purchased from Envigo RMS SRL (S. Pietro al Natisone, UD, Italy). Animals were acclimatized for one week before treatment in the animal room set to maintain controlled temperature (22 ± 3 °C) and humidity (50–60%), in presence of a fixed artificial light cycle with 12 h light (7:00 a.m. – 7:00 p.m.) and 12 h dark (7:00 p.m. – 7:00 a.m.). Mice were caged in groups of 4 animals, using dust-free poplar chips for bedding and fed with a standard diet for rodents. Water and feed were provided *ad libitum* during all phases of the study. Experiments were carried out at the University of Trieste in conformity with the Italian law decree (D.L.) n. 26 of 4th March 2014 and associated guidelines of the European Union on the protection of animals used for scientific purposes (Directive 2010/63/EU of the European Parliament and of the Council of 22nd September 2010). Experiments were approved by the University Body for Animal Well-being (OPBA) of the University of Trieste and by Italian Ministry of Health (authorization n° 296/2017-PR).

2.3. Local Lymph Node Assay: BrdU-ELISA (OECD TG 442B)

Skin sensitization properties of FLG and GO were evaluated following the specific OECD TG 442B, namely the Local Lymph Node Assay (LLNA): BrdU-ELISA (OECD, 2018). It consists in a non-radioactive modification of the LLNA test method, which uses non-radiolabeled 5-bromo-2-deoxyuridine (BrdU) in an ELISA-based test system to measure lymphocyte proliferation, therefore measuring the last phase of skin sensitization Adverse Outcome Pathway (AOP) (OECD, 2010).

Animals (4 for each treatment group) were randomly selected and kept in their cages for one week prior to the start of dosing to allow their acclimatization. FLG or GO were dispersed in polyethylene glycol (PEG) 60% (*w*/w in distilled water), chosen among the buffers suggested by the OECD TG 442B, being able to maintain stable GBM dispersions. FLG or GO dispersions (25 μL) were daily applied to the dorsum of both ears of mice, for three consecutive days (days 0–2), at three doses: 0.4, 4.0 and 40 mg/mL (equal to 0.01, 0.10 and 1.00 mg/ear). Being a nanomaterial, FLG and GO have been considered as solid test substances to be suspended as a slurry for guaranteeing that after their application on mice ears they are not removed, for instance by rubbing, considering their fluffy lightweight nature. Therefore, the dose choice was based on the maximum possible concentration for these solids in suspensions to obtain slurries easily applicable on mice ears while avoiding their removal. The negative control group was exposed to vehicle (60% PEG) whereas positive control groups were exposed to 25% eugenol or 1% 2,4-dinitrochlorobenzene (DNCB). On day 4 (48 h after the last treatment), all mice were intraperitoneally (i.p) injected with 500 μL sterile BrdU solution (10 mg/mL; equal to 5 mg BrdU/mouse) and after 24 h (day 5), mice were sacrificed by CO_2 euthanasia to collect their auricular lymph nodes.

From each mouse, a single-cell suspension from bilateral lymph nodes was prepared by gentle mechanical disaggregation using a disposable plastic pestle to crush the lymph nodes, followed by passage through a #70 nylon mesh (Corning; Milan, Italy) and cells suspension in 15 mL phosphate buffered saline (PBS). Lymph node cells (LNC) proliferation was then quantified as BrdU incorporation using the BrdU

Table 1
Physicochemical properties of FLG and GO as previously reported for the same batches of materials (Fusco et al., 2020a; Cavion et al., 2020).

GBMs	Elemental Analysis ± SD (%)					TGA weight loss (%)[a]	Lateral dimension ± SD (nm)	Lateral dimension distribution (nm)	n° layers
	C	H	N	S	O				
FLG	94.93 ± 0.28	0.55 ± 0.02	0.54 ± 0.02	0.32 ± 0.03	<3.7	6	171 ± 147[b]	50-600[b]	4[d]
GO	59.40 ± 0.10	1.40 ± 0.10	0.07 ± 0.02	2.92 ± 0.52	<36.6	58	15,100 ± 400[c]	6000-30000[c]	6[e]

FLG: few-layer graphene; GO: graphene oxide; TGA: thermogravimetric analysis; SD: standard deviation.
[a] Values determined at 600 °C.
[b] Value determined by TEM on at least 100 sheets.
[c] Values determined by laser diffraction in the GO slurry.
[d] Value determined according to Paton et al., 2014.
[e] Value determined by X-ray diffraction (XRD) analysis.

Cell Proliferation Assay (Sigma-Aldrich; Milan, Italy), according with the manufacturer's instructions. Briefly, LNC suspensions (100 µL) were added in triplicate in each well of a flat-bottom 96-well microplates. After LNC fixation and denaturation, peroxidase-conjugated anti-BrdU antibody was added; after washing, the substrate solution was added and the absorbance was read at 450 nm using the FLUOstar Omega Automated Microplate Reader (Bio-Tek Instruments GmbH; Bad Friedrichshall, Germany) to calculate the BrdU-labeling index of each sample. Stimulation index (SI) was then calculated by dividing the BrdU-labeling index of each test group by that of the vehicle control group. In accordance to the OECD TG 442B, the criteria for considering positiveness of the results relies on SI values ≥1.6, therefore predicting skin sensitization properties.

2.4. Clinical observations

Animal were carefully checked for signs of toxicity during all the experiment period. In particular, body weight as well as feed and water consumption were daily monitored. In addition, other signs of toxicity were daily recorded.

Ear edema formation was monitored by ear thickness measurements using a digital micrometer (Mitutoyo Inc.; Tokyo, Japan) on Day 0 (pre-dose), Day 2 (48 h after the first dose) and Day 5. On Day 5, edema was measured also after euthanasia by ear punch (Ø 6 mm) weight using an analytical balance. In each mouse, edema was expressed as mean value from the two bilateral measurements. In parallel, signs of skin irritation were evaluated by visual inspection following the erythema scoring reported in the OECD TG 442B.

2.5. Histological analysis

Ear biopsies, fixed in 10% formalin, were dehydrated in ascending grades of ethanol, cleared in xylene, and embedded in paraffin wax. Sections (20 µm) were stained with hematoxylin-eosin or Giemsa stain, and observed using an inverted light Leica DMi1 microscope equipped with a FLEXACAM C1 standard camera (Leica Microsystems; Milan, Italy).

2.6. Myeloperoxidase activity

Myeloperoxidase activity was quantified as previously described (Giangaspero et al., 2009) as index of neutrophilic granulocytes infiltrate to measure the inflammatory response, in the same ear plug used to evaluate edema formation. Briefly, each ear plug, suspended in 1 mL buffered saline (0.1 M sodium acetate buffer at pH 4.2), containing 0.1% (*w/v*) hexadecyltrimethylammonium bromide (HTAB), was homogenized by Ultra-Turrax (Ika-Werk; Staufen, Germany) for 5 s at 20,000 rpm. The homogenate was centrifuged at 15,000 *g* for 5 min, and 25 µL of the supernatant were added to each well of a flat-bottom 96-well microplate. Then, the supernatant was mixed with 50 µL of the chromogen solution [2.83 mM 3,3′,5,5′-tetramethylbenzidine (TMB) dissolved in 0.1 M sodium acetate buffer at pH 4.2, containing 0.1% (w/v) HTAB]. The enzyme reaction was started adding 75 µL of 0.7 mM hydrogen peroxide and, after 5 min incubation at 25 °C, it was blocked by 50 µL of 4 M acetic acid, containing 10 mM sodium azide. The absorbance was read at 620 nm using the FLUOstar Omega Automated Microplate Reader (Bio-Tek Instruments GmbH; Bad Friedrichshall, Germany). Myeloperoxidase activity was expressed as enzyme units in 1 mL supernatant. One unit of myeloperoxidase activity (U) was defined as the amount of enzyme oxidizing 1 nmol TMB/min. The enzyme activity of each sample was determined in duplicate.

2.7. Statistical analysis

Skin sensitization prediction was evaluated in compliance with the OECD TG 442B, considering positive criteria for SI values ≥1.6 as positive threshold response for sensitizers. Negative criteria (SI < 1.6) and borderline criteria (SI between 1.6 and 1.9) were also considered, as suggested by the OECD TG 442B. Edema and myeloperoxidase activity data are expressed as mean ± standard error (SE) of at least 3 independent measurements. Data were analyzed by a one-way analysis of variance (ANOVA) followed by Bonferroni's post-test (GraphPad Prism software, version 6) with significant differences for $p < 0.05$.

3. Results

3.1. Skin sensitization potential of FLG and GO

Skin sensitization potential of FLG and GO was evaluated in female CBA/JN mice according to the OECD TG 442B, by 3-day cutaneous exposure to each of three doses of the materials dispersed in 60% PEG (0.4, 4.0 and 40 mg/mL, equal to 0.01, 0.10 and 1.00 mg/ear). Prediction of skin sensitization was based on SI calculated in LNC collected from the auricular lymph nodes 3 days after the last treatment. Fig. 1 shows the mean SI calculated for FLG- or GO-treated mice in comparison to that of the untreated control group (vehicle) as well as the mean SI value for the two positive controls (mice exposed to 25% eugenol or to 1% DNCB). SI values measured in LNC from all the FLG- or GO-treated mice were lower than 1.6, regardless the dose, which suggests that both materials are not skin sensitizers. As expected, eugenol, and to a greater extent DNCB, significantly increased SI at 2.4 ± 0.6 ($p < 0.05$) and 3.9 ± 0.5 ($p < 0.01$), respectively, which confirm their skin sensitization properties.

3.2. Clinical observations

All throughout the experiment, animals were checked for any clinical sign of toxicity. In general, no behavioral changes or other changes indices of altered neuromuscular, respiratory or cardiac activities were noticed in all the groups of treatment. Fig. 2 shows the mean body

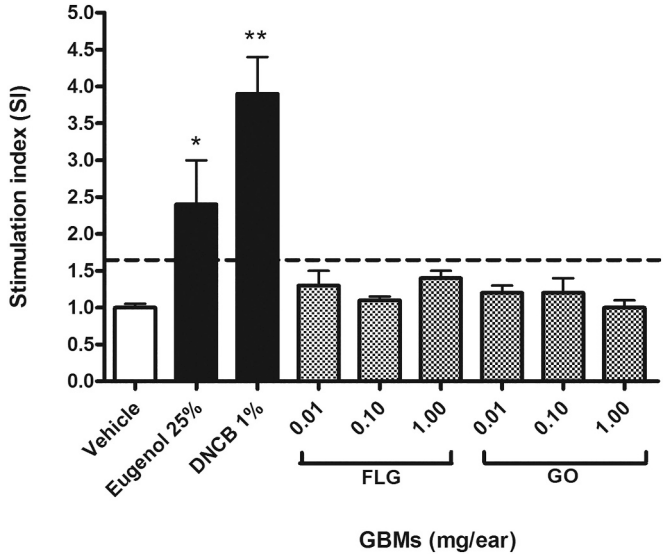

Fig. 1. Prediction of skin sensitization potential of FLG and GO according to the OECD TG 442B, expressed as stimulation index (SI) for LNC collected from auricular lymph nodes 3 days after the last treatment (doses: 0.01, 0.10 and 1.00 mg/ear). The dashed line represents the threshold set by the guideline above which skin sensitization prediction is positive. As positive control, mice were exposed to 25% eugenol or 1% DNCB, whereas negative control consisted in mice exposed to the vehicle (60% PEG). Statistical analysis *vs* vehicle to determine the significance of prediction: *, $p < 0.05$; **, $p < 0.01$ (One-way ANOVA and Bonferroni's post-test).

weight data of mice treated with each dose of FLG (panel A) or GO (panel B), in comparison to those of negative (vehicle; 60% PEG) or positive (25% eugenol or 1% DNCB) controls. No reduction of body weight was recorded in each group of treatment as compared to negative control. Individual weights of mice at start of dosing and at scheduled humane kill as well as mean and associated error terms for each treatment group are reported in Supplementary fig. 2. Similarly, no changes in feed consumption were recorded (data not shown).

At the end of the experiment, edema was measured on euthanized animals by the mean weight of a punch (Ø 6 mm) from the two ears' pinna. Fig. 3 shows the mean weight of the ear punches from mice exposed to each dose of FLG or GO, in comparison to that of negative (vehicle; 60% PEG) or positive (25% eugenol or 1% DNCB) controls. No increase of ear weight as index of edema formation was recorded in mice exposed to FLG or GO for all the treatment, suggesting the lack of irritation or inflammation for both materials. On the other hand, only 1% DNCB induced edema formation, increasing the ear punch weight by 2.8 folds as compared to the negative control. Similar results were obtained measuring ear pinna thickness at Day 0 (pre-dose), Day 2 (48 h after the first exposure) and Day 5 (at the end of experiment): exposure to FLG or GO did not increase ear pinna thickness due to oedema formation, whereas only 1% DNCB induced a significant thickness increase at Days 2 and 5 (Supplementary Fig. 1).

Irritation potential was also evaluated at the end of the experiment (Day 5: 3 days after the last treatment) by erythema scoring, as reported by the OECD TG 442B (OECD, 2018). On the basis of visual inspections performed on mice after sacrifice (Supplementary fig. 3), only mice exposed to 1% DNCB showed signs of moderate-to-sever erythema on the ear dorsal part (erythema score = 3), whereas no signs of erythema were noticed in mice exposed to the other substances or to vehicle (erythema score = 0; Table 2).

3.3. Histological analysis

The potential pro-inflammatory effect of FLG and GO was further evaluated by histological analysis of ear biopsies from euthanized mice (Day 5). Negative control (vehicle) displayed a regular tissue organization in the ear pinna with (1) the thin epidermis, visible as dark pink tissue formed by multiple layers of flattened cells on the ventral and the dorsal surface of the ear pinna; (2) the dermis, visible as thicker

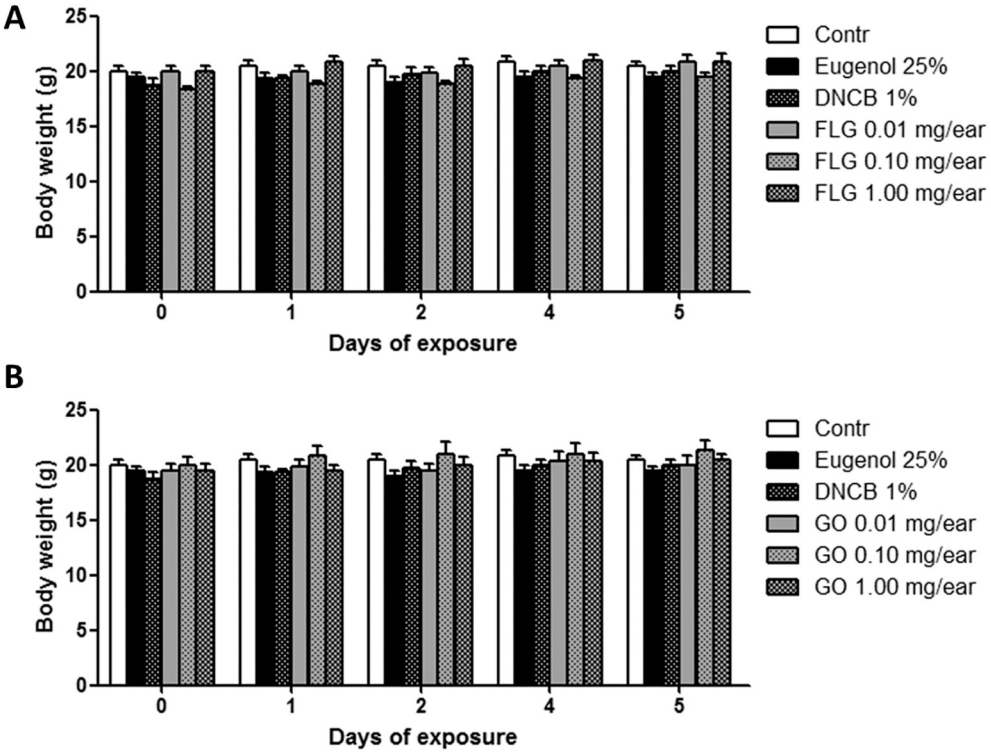

Fig. 2. Mean body weight (g) of mice ($n = 4$) exposed to FLG (A) or GO (B) in comparison to the negative control (vehicle; 60% PEG) and positive controls (25% eugenol or 1% DNCB) during the experiment period.

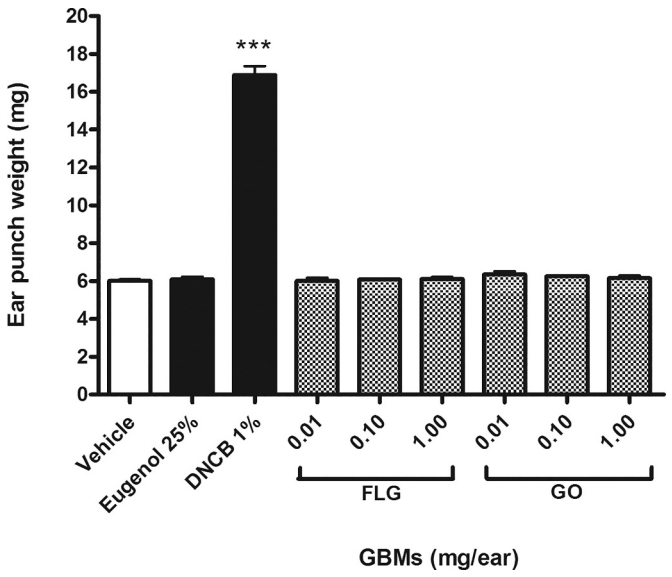

Fig. 3. Mean ear pinna punch weight (mg) of mice ($n = 4$) exposed to FLG or GO (0.01, 0.10 or 1.00 mg/ear) in comparison to that of the negative control (vehicle; 60% PEG) and positive controls (25% eugenol or 1% DNCB) at Day 5 (3 days after the last treatment). Statistical analysis *vs* vehicle: ***, $p < 0.001$ (One-way ANOVA and Bonferroni's post-test).

Table 2
Erythema scores by visual inspections in compliance with the OECD TG 442B performed at Day 5 (3 days after the last treatment).

Treatment group	Observation	Erythema score	Incidence of erythema[a]
Vehicle	No erythema	0	–
Eugenol 25%	No erythema	0	–
DNCB 1%	Moderate to severe erythema	3	4/4
FLG (0.01 mg/ear)	No erythema	0	–
FLG (0.10 mg/ear)	No erythema	0	–
FLG (1.00 mg/ear)	No erythema	0	–
GO (0.01 mg/ear)	No erythema	0	–
GO (0.10 mg/ear)	No erythema	0	–
GO (1.00 mg/ear)	No erythema	0	–

[a] Number of animals with erythema/total animals.

connective tissue below the epidermis, with scattered purple stained cell nuclei; (3) a cartilage layer (clear white circles) at approximately 1/3 of the distance between the ventral and dorsal epidermis layers. The ear pinna of positive controls exposed to 25% eugenol did not show any significant morphological skin alterations. On the contrary, 1% DNCB induced degeneration of epidermis and infiltration of neutrophilic granulocytes, evidenced as increased number of cells containing purple stained nuclei, especially in the dermis at contact with dorsal epidermis. After exposure to FLG- or GO, neither significant morphological skin tissues alteration nor infiltration of inflammatory cells was observed. However, black-brownish depots were observed above and within the epidermis of mice exposed to FLG, and in the dermis of those exposed to GO (Fig. 4).

To further assess the presence of GBM depot within the ear pinna skin, sections were observed at 40× magnification. As depicted in Fig. 5, brownish dots were observed in the ear tissues of mice exposed to FLG or GO, but not in those of negative or positive controls. In particular, GBM agglomerates/aggregates were noted above the epidermis (especially after exposure to FLG) and small depots localized between cells of the dorsal dermis (after exposure to FLG or GO).

3.4. Myeloperoxidase activity

The pro-inflammatory potential by skin exposure to FLG or GO was evaluated also quantifying the neutrophilic granulocytes infiltrate through the measurement of myeloperoxidase activity in the ear punch of mice at Day 5. As shown by Fig. 6, both FLG and GO did not induce any significant increase of myeloperoxidase activity in the ear pinna with respect to the negative control (vehicle). On the contrary, 25% eugenol or 1% DNCB significantly increased the enzyme activity from 5.3 ± 0.3 U/mL x min (negative control) to 7.6 ± 0.8 U/mL x min (43% increase; $p < 0.05$) and 21.8 ± 4.4 U/mL x min (311% increase; $p < 0.01$), respectively.

4. Discussion

Among the various types of carbon-based nanomaterials, GBMs have attracted remarkable attention due to their versatile applications in different technological fields, leading to an increased production, but also raising concerns about their harmful potential to humans and the environment (Fadeel et al., 2018; Xiaoli et al., 2020; Ding et al., 2022). Exposure to GBMs occurs mainly by occupational-related routes during manufacturing procedures and the intentional ones associated with particular technological applications of these materials. In this scenario, skin contact is one of the most feasible routes of exposure to GBMs, but also one of the most underestimated (Pelin et al., 2018a; Chen et al., 2020).

With the aim to characterize the hazard posed by GBMs at the cutaneous level, a series of *in vitro* studies on keratinocytes (*i.e.* HaCaT cells) has been previously carried out on selected materials. The mechanism of GBM toxicity toward HaCaT cells seems to be related to a reduced mitochondrial activity associated with their sustained interaction with plasma membrane (Pelin et al., 2017). Moreover, both FLG and GO induced a concentration- and time-dependent ROS production in HaCaT cells, GO being slightly more toxic than FLG, tentatively through flavoprotein-based enzymes (NADH dehydrogenase and xanthine oxidase) activation (Pelin et al., 2018b), leading to a metabolic rearrangement due to a compromised mitochondrial function (Frontiñán-Rubio et al., 2018). Metabolome remodeling was noticed in keratinocytes also after 1-week exposure to sub-cytotoxic concentrations of FLG, with alterations in the cellular energetic metabolism, calcium ions and redox homeostasis (Frontiñan-Rubio et al., 2020). Intriguingly, the cytotoxic effects of FLG and GO toward HaCaT keratinocytes seem to be only partially reversible after their withdrawal, an important aspect for the hazard characterization of skin devices containing GBMs (Pelin et al., 2020).

Quite recently, we also demonstrated that HaCaT cells exposed to sub-cytotoxic concentrations (0.01–1.0 μg/mL) of endotoxin-free FLG or thermally dehydrated GO (d-GO) released pro-inflammatory cytokines (*e.g.*, IL-1α, IL-6, IL-8 and TNF-α), suggesting keratinocytes ability to sense GBMs even at very low concentrations. However, conditioned media collected from GBM-treated keratinocytes were unable to influence monocytes differentiation and migration, two crucial events in inflammatory and immune responses involving activated monocytes. In particular, even though the study was not aimed at assessing GBM skin sensitization potential, the lack of monocyte differentiation seems to argue against a sensitization potential of these materials (Fusco et al., 2020b).

Hence, to verify the absence of skin sensitization potential of FLG and GO, two of the main representative GBMs, this study was carried out following the specific OECD TG 442B and, in particular, using the LLNA: BrdU-ELISA procedure. This is a stand-alone OECD TG able to predict the fourth key event of skin sensitization AOP, namely lymphocytes

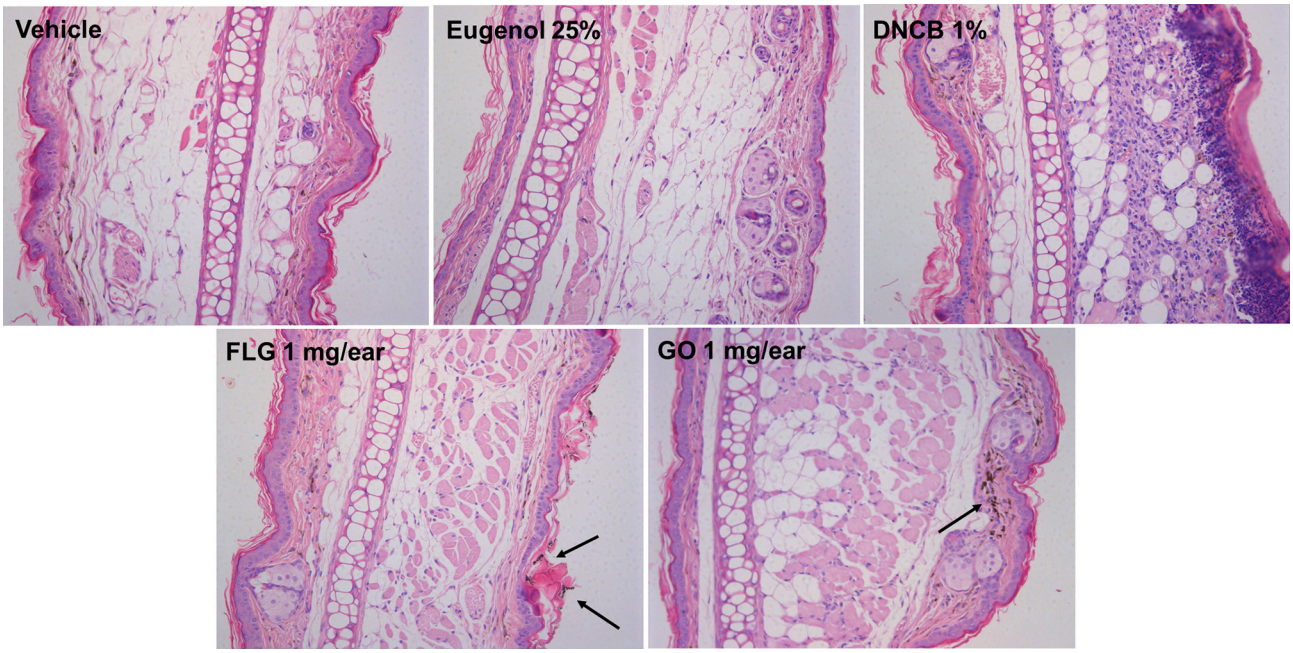

Fig. 4. Light micrographs of mice ear pinna at Day 5: 3 days after the last exposure to the vehicle (60% PEG; negative control), 25% eugenol or 1% DNCB (positive controls), or the highest dose of FLG or GO (40 mg/mL; 1.00 mg/ear). Black arrows show black/brownish depots of GBMs. Hematoxylin and eosin stain. Magnification: 20×.

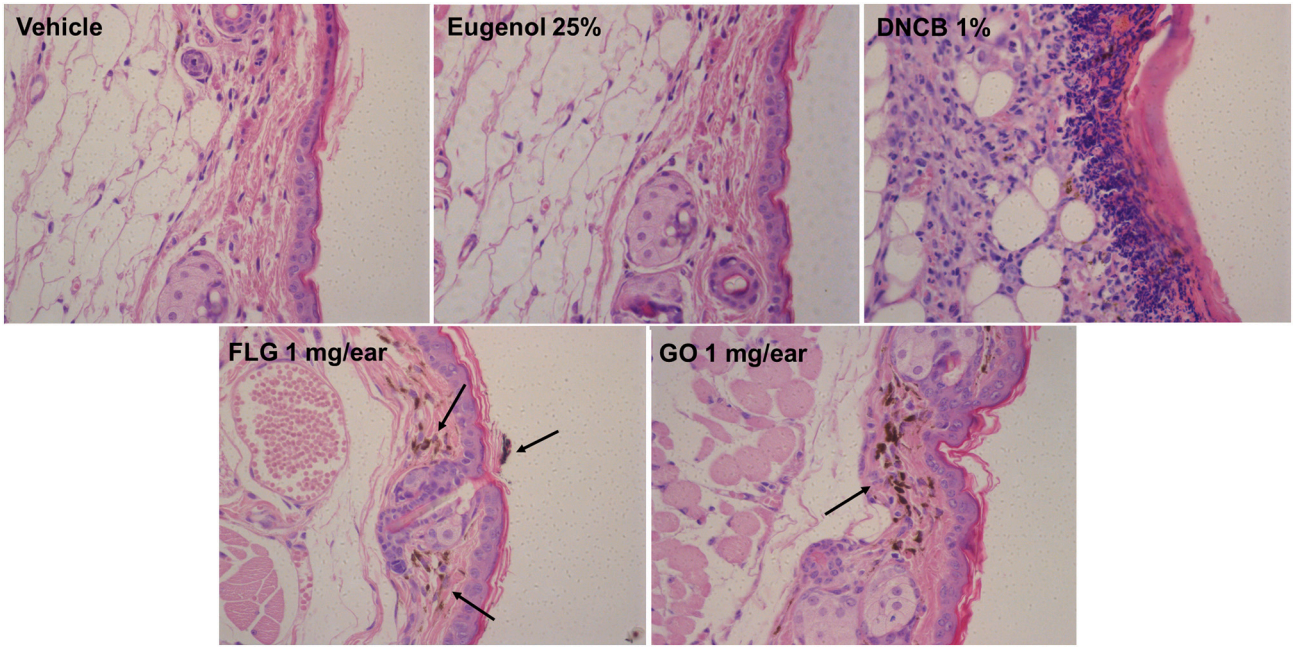

Fig. 5. Light micrographs of mice ear pinna at Day 5: 3 days after the last exposure to the vehicle (60% PEG; negative control), 25% eugenol or 1% DNCB (positive controls), or the highest dose of FLG or GO (40 mg/mL; 1.00 mg/ear). Black arrows show black/brownish depots of GBMs above the epidermis and/or within the dermis. Hematoxylin and eosin stain. Magnification: 40×.

activation (OECD, 2010). In contrast, the three *in vitro* OECD TG able to predict the first three AOP key events (peptide reactivity, keratinocytes and dendritic cells activation) cannot be used as stand-alone TG and, therefore, must be applied together to predict a skin sensitization potential (OECD TG 497; OECD, 2021). In particular, the LLNA:BrdU-ELISA procedure consists of an *in vivo* method on a limited number of animals as compared to the previously available tests on guinea pigs (OECD TG 406), refined in the way by which animals are used for allergic contact sensitization testing, in compliance with the 3Rs principle (OECD, 2018). The assay uses a non-radioactive procedure to predict skin sensitization potential by evaluating the fourth key event of skin sensitization pathway, namely the proliferation of lymphocytes in the local lymph nodes draining the site of test substance application (mice ears pinna). An increased lymphocytes proliferation expressed as SI $\geq$ 1.6-fold with respect to untreated controls is a predictive index of skin sensitizers (OECD, 2018). In our study, SI of both FLG and GO were lower than the threshold limit of 1.6 and, consequently, these GBMs can be considered as non-skin sensitizers, in contrast to eugenol and DNCB

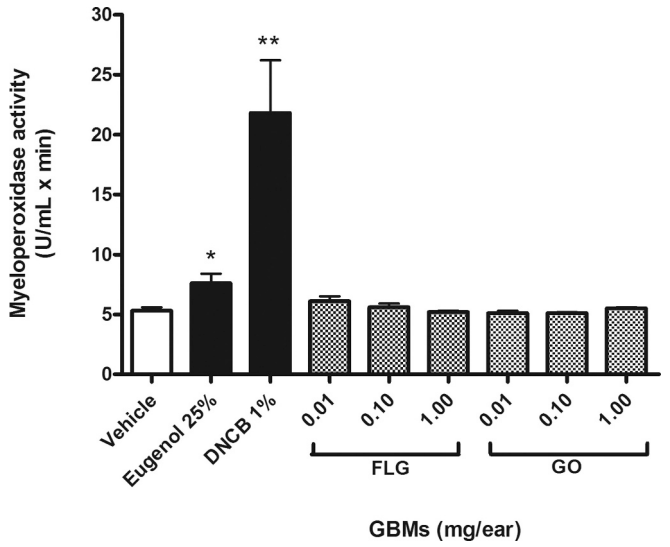

Fig. 6. Myeloperoxidase activity (U/mL x min) in the ear pinna punch of mice ($n = 4$) exposed to FLG or GO (0.01, 0.10 and 1.00 mg/ear) in comparison to that of the negative control (vehicle; 60% PEG) and positive controls (25% eugenol or 1% DNCB) at Day 5 (3 days after the last exposure). Statistical analysis *vs* vehicle: *, $p < 0.05$; **, $p < 0.01$ (One-way ANOVA and Bonferroni's post-test).

used as positive controls. This finding is in line with the records of a very recent study on graphene nanoplatelets (GNP) suggesting the lack of skin sensitization properties (Kim et al., 2021), even though the actual GNP doses were not clearly stated. Notwithstanding, the results of our study suggest that the two kinds of GBMs are non-sensitizers after skin exposure, including GO which could highly react with host skin proteins, in view of its higher content of reactive O_2-bearing groups as compared to FLG or GNP.

As suggested by OECD TG 442B, the study was implemented by the evaluation of additional adverse effects, including clinical signs of general toxicity (*i.e.* body weight, water and feed consumption, changes in behavior, neuromuscular, cardiac and respiratory functions) and skin toxicity (edema and erythema induction). Our results demonstrate that neither FLG nor GO influenced the body weight and feed consumption with respect to negative controls. Similarly, no signs of edema and erythema were noted, suggesting the absence of skin irritation or inflammation. Lack of skin inflammation was further confirmed by histological analysis and the measurement of myeloperoxidase activity in ear pinna biopsies as index of neutrophilic granulocytes infiltrate. In particular, histological analysis of ear biopsies from mice exposed to FLG or GO did not show any tissue alteration or inflammatory cells infiltration in the skin. The latter was confirmed quantifying myeloperoxidase activity. As expected, the positive control DNCB induced a visible erythema and edema, with tissues alterations and infiltration of inflammatory cells observable by light microscopy.

The histological analysis of ear biopsies from mice exposed to FLG or GO revealed the presence of black/brownish dots above and within the dorsal ear epidermis (FLG) and between cells of the dermis (FLG, GO). These dots can be referred as small depots of FLG or GO, even though we cannot exclude that those present at the dermis-epidermis junction level could consist also in melanin granules. Nevertheless, as these dark dots were not observed in negative or positive controls, it is likely that they consist in FLG or GO deposits. This observation is of particular importance, since it suggests that, even in the absence of skin sensitization, irritation and inflammation, FLG and GO can penetrate into the dermis. This finding is consistent with previous observations on other related carbon-based materials, such as C60 fullerenes, able to penetrate through the epidermis without inducing signs of irritation or sensitization in animals (Xia et al., 2010; Dalla Colletta et al., 2022). At best of our knowledge, this is the first *in vivo* evidence of a possible GBM penetration into the dermis, corroborating a recent study demonstrating skin permeation of GO (about 55% of the total GO, after 6 h contact) using Franz diffusion cells (Silva et al., 2021). Other *in vitro* evidences suggested the capability of different GBMs to penetrate into keratinocytes and fibroblasts (Liao et al., 2011; Li et al., 2013; Pelin et al., 2018a, 2018b; Pelin et al., 2020). Most importantly, recovery analysis performed exposing HaCaT keratinocytes to FLG for 24 h followed by the material withdrawal for 48 h demonstrated the presence of FLG particles inside keratinocytes at the end of the recovery period (Pelin et al., 2020). This observation suggests that internalized FLG is retained by cells over time; therefore, we cannot exclude possible accumulation of GBMs and consequent long-term detrimental effects at the skin level.

In addition, it is noteworthy that one of the main drawbacks of nanosafety studies, often reducing the quality of toxicological data, relies on an incomplete physico-chemical characterization of the studied nanomaterial, beside an incomplete description of the experimental design, including the animal characteristics (*i.e.* species, gender, weight, age, *etc.*) (Fernández-Cruz et al., 2018). All these information have been considered to define a scoring system following the principles of the Klimisch score (K score), providing a comprehensive criteria and guidance for reliability evaluations of toxicological data (Schneider et al., 2009). K score analysis is freely available through the ToxRTool (https://joint-research-centre.ec.europa.eu/scientific-tools-and-databases/toxrtool-toxicological-data-reliability-assessment-tool_en) through which application, the present study resulted in a score of 20 out of 21, indicating our study in the Klimisch category 1 (reliable without restrictions), therefore highlighting the reliability of the data.

In conclusion, this *in vivo* toxicological study following the OECD TG 442B demonstrates the absence of skin sensitization properties for two representatives of GBMs, FLG and GO. Beside the lack of skin sensitization properties, both FLG and GO seem unable to induce skin irritation and inflammation, despite their capability to slightly penetrate into the dermis. Overall, these results represent a significant step forward in the characterization of the hazard posed by GBM at the skin level, still incomplete (Dalla Colletta et al., 2022). Indeed, it should be noted that a registration dossier for graphene is currently present at the European Chemical Agency (ECHA), in which toxicological data on skin sensitization rely only on a non-referred study based on Buelher test on guinea pigs, following the OECD TG 406 version adopted in 1992 (https://echa.europa.eu/it/registration-dossier/-/registered-dossier/24678). Even though a recent revision and correction of this TG has been done in 2022 (OECD, 2022), it should be noted that the OECD TG 406 involves the intradermal administration of the test substance, which effects may be heavily different than those induced by a topical exposure, as in the case of our study. Hence, on the whole, the results of this study acquire a significant importance for the assessment of the risk associated with GBM skin exposure, in particular for workers and consumers in case of GBM-enriched devices directly in contact with the skin.

Financial support

This study was supported by the European Commission Graphene Flagship Core 3 (grant agreement no. 881603). Part of this work was performed under the Maria de Maeztu Units of Excellence Program from the Spanish State Research Agency – Grant No. MDM-2017-0720. Prof. M. Prato is recipient of the Carbon Bionanotechnology AXA Chair (2016-2023). Financial support from The Spanish Ministry of Science and Innovation, Grant PID2019-104381GB-I00 is also acknowledged.

Authors are grateful to Beneficentia Stiftung Foundation (Liechtenstein) for the financial support for the purchase of the FLUOstar Omega instrument, necessary for the analysis carried out in this study.

CRediT authorship contribution statement

Silvio Sosa: Conceptualization, Investigation, Formal analysis,

Writing – review & editing. **Aurelia Tubaro:** Conceptualization, Writing – review & editing. **Michela Carlin:** Investigation, Formal analysis. **Cristina Ponti:** Investigation. **Ester Vázquez:** Investigation, Resources. **Maurizio Prato:** Funding acquisition, Supervision. **Marco Pelin:** Investigation, Formal analysis, Supervision, Writing – original draft.

Declaration of Competing Interest

The authors declare that they have no known competing financial interests or personal relationships that could have appeared to influence the work reported in this paper.

Data availability

Data will be made available on request.

Appendix A. Supplementary data

Supplementary data to this article can be found online at https://doi.org/10.1016/j.impact.2022.100448.

References

Bianco, A., Cheng, H.M., Enoki, T., Gogotsi, Y., Hurt, R.H., Koratkar, N., Kyotani, T., Monthioux, M., Park, C.R., Tascon, J.M.D., Zhang, J., 2013. All in the graphene family - a recommended nomenclature for two-dimensional carbon materials. Carbon 65, 1–6. https://doi.org/10.1016/j.carbon.2013.08.038.

Cavion, F., Fusco, L., Sosa, S., Manfrin, C., Alonso, B., Zurutuza, A., Della Loggia, R., Tubaro, A., Prato, M., Pelin, M., 2020. Ecotoxicological impact of graphene oxide: toxic effects on the model organism *Artemia franciscana*. Env. Sci. Nano 7, 3605–3615. https://doi.org/10.1039/D0EN00747A.

Chen, L., Li, J., Chen, Z., Gu, Z., Yan, L., Zhao, F., Zhangl, A., 2020. Toxicological evaluation of graphene family nanomaterials. J. Nanosci. Nanotechnol. 20 (4), 1993–2006. https://doi.org/10.1166/jnn.2020.17364.

Dalla Colletta, A., Pelin, M., Sosa, S., Fusco, L., Prato, M., Tubaro, A., 2022. Carbon-based nanomaterials and skin: an overview. Carbon 196, 683–698. https://doi.org/10.1016/j.carbon.2022.05.036.

Ding, X., Pu, Y., Tang, M., Zhang, T., 2022. Environmental and health effects of graphene-family nanomaterials: potential release pathways, transformation, environmental fate and health risks. Nano Today 42, 101379. https://doi.org/10.1016/j.nantod.2022.101379.

Eedy, D.J., 1996. Carbon-fibre-induced airborne irritant contact dermatitis. Contact Dermatitis 35 (6), 362–363. https://doi.org/10.1111/j.1600-0536.1996.tb02418.x.

Erf, G.F., Falcon, D.M., Sullivan, K.S., Bourdo, S.E., 2017. T lymphocytes dominate local leukocyte infiltration in response to intradermal injection of functionalized graphene-based nanomaterial. J. Appl. Toxicol. 37 (11), 1317–1324. https://doi.org/10.1002/jat.3492.

Fadeel, B., Cyrill, B., Merino, S., Vazquez, E., Flahaut, E., Mouchet, F., Lauris, E., Laury, G., Koivisto, A.J., Vogel, U., Martín, C., Delogu, L.G., Buerki-Thurnherr, T., Wick, P., Beloin-Saint-Pierre, D., Hischier, R., Pelin, M., Candotto Carniel, F., Tretiach, M., Cesca, F., Benfenati, F., Scaini, D., Ballerini, L., Kostarelos, K., Prato, M., Bianco, A., 2018. Safety assessment of graphene-based materials: focus on human health and the environment. ACS Nano 12, 10582–10620. https://doi.org/10.1021/acsnano.8b04758.

Fernández-Cruz, M.L., Hernández-Moreno, D., Catalán, J., Cross, R.K., Stockmann-Juvala, H., Cabellos, J., Lopes, V.R., Matzke, M., Ferraz, N., Izquierdo, J.J., Navas, J. M., Park, M., Svendseng, C., Janer, G., 2018. Quality evaluation of human and environmental toxicity studies performed with nanomaterials – the GUIDEnano approach. Environ. Sci.: Nano 5, 381–397. https://doi.org/10.1039/C7EN00716G.

Frontiñán-Rubio, J., Gómez, M.V., Martín, C., González Domínguez, J.M., Durán-Prado, M., Vázquez, E., 2018. Differential effects of graphene materials on the metabolism and function of human skin cells. Nanoscale 10 (24), 11604–11615. https://doi.org/10.1039/C8NR00897C.

Frontiñan-Rubio, J., Gomez, M.V., González, V.J., Durán-Prado, M., Vázquez, E., 2020. Sublethal exposure of small few-layer graphene promotes metabolic alterations in human skin cells. Sci. Rep. 10 (1), 18407. https://doi.org/10.1038/s41598-020-75448-0.

Fusco, L., Garrido, M., Martín, C., Sosa, S., Ponti, C., Centeno, A., Alonso, B., Zurutuza, A., Vázquez, E., Tubaro, A., Prato, M., Pelin, M., 2020a. Skin irritation potential of graphene-based materials using a non-animal test. Nanoscale 12, 610–622. https://doi.org/10.1039/c9nr06815e.

Fusco, L., Pelin, M., Mukherjee, S., Keshavan, S., Sosa, S., Martín, C., González, V., Vázquez, E., Prato, M., Fadeel, B., Tubaro, A., 2020b. Keratinocytes are capable of selectively sensing low amounts of graphene-based materials: implications for cutaneous applications. Carbon 159, 598–610. https://doi.org/10.1016/j.carbon.2019.12.064.

Geetha Bai, R., Muthoosamy, K., Manickam, S., Hilal-Alnaqbi, A., 2019. Graphene-based 3D scaffolds in tissue engineering: fabrication, applications, and future scope in liver tissue engineering. Int. J. Nanomedicine 14, 5753–5783. https://doi.org/10.2147/IJN.S192779.

Geim, A.K., Novoselov, K.S., 2007. The rise of graphene. Nat. Mater. 6, 183e91. https://doi.org/10.1038/nmat1849.

Giangaspero, A., Ponti, C., Pollastro, F., Del Favero, G., Della Loggia, R., Tubaro, A., Appendino, G., Sosa, S., 2009. Topical anti-inflammatory activity of wupatilin, a lipophilic flavonoid from mountain wormwood (*Artemisia umbelliformis* Lam.). J. Agric. Food Chem. 57, 7726–7730. https://doi.org/10.1021/jf901725p.

Guo, X., Mei, N., 2014. Assessment of the toxic potential of graphene family nanomaterials. J. Food Drug Anal. 22 (1), 105–115. https://doi.org/10.1016/j.jfda.2014.01.009.

Ho, D.H., Sun, Q., Kim, S.Y., Han, J.T., Kim, D.H., Cho, J.H., 2016. Stretchable and multimodal all graphene electronic skin. Adv. Mater. 28 (13), 2601–2608. https://doi.org/10.1002/adma.201505739.

Karim, N., Afroj, S., Tan, S., He, P., Fernando, A., Carr, C., Novoselov, K.S., 2017. Scalable production of graphene-based wearable E-textiles. ACS Nano 11 (12), 12266–12275. https://doi.org/10.1021/acsnano.7b05921.

Kasparov, A.A., Popova, T.B., Lebedeva, N.V., Gladkova, E.V., Gurvich, E.B., 1989. Evaluation of the carcinogenic hazard in the manufacture of graphite articles. Vopr. Onkol. 35 (4), 445–450.

Kenry, Loh K.P., Lim, C.T., 2016. Molecular interactions of graphene oxide with human blood plasma proteins. Nanoscale 8 (17), 9425–9441. https://doi.org/10.1039/c6nr01697a.

Kim, J., Lee, J., Son, D., Choi, M.K., Kim, D.H., 2016. Deformable devices with integrated functional nanomaterials for wearable electronics. Nano Converg. 3, 4. https://doi.org/10.1186/s40580-016-0062-1.

Kim, S.H., Hong, S.H., Lee, J.H., Lee, D.H., Jung, K., Yang, J.Y., Shin, H.S., Lee, J., Jeong, J., Oh, J.H., 2021. Skin sensitization evaluation of carbon-based graphene nanoplatelets. Toxics 9 (3), 62. https://doi.org/10.3390/toxics9030062.

Kotagiri, N., Kim, J.W., 2014. Stealth nanotubes: strategies of shielding carbon nanotubes to evade opsonization and improve biodistribution. Int. J. Nanomedicine 9 (Suppl. 1), 85–105. https://doi.org/10.2147/IJN.S51854.

León, V., Quintana, M., Herrero, M.A., Fierro, J.L., de la Hoz, A., Prato, M., Vázquez, E., 2011. Few-layer graphenes from ball-milling of graphite with melamine. Chem. Commun. (Camb.) 47 (39), 10936–10938. https://doi.org/10.1039/c1cc14595a.

León, V., Rodriguez, A.M., Prieto, P., Prato, M., Vázquez, E., 2014. Exfoliation of graphite with triazine derivatives under ball-milling conditions: preparation of few-layer graphene via selective noncovalent interactions. ACS Nano 8 (1), 563–571. https://doi.org/10.1021/nn405148t.

León, V., González-Domínguez, J.M., Fierro, J.L., Prato, M., Vázquez, E., 2016. Production and stability of mechanochemically exfoliated graphene in water and culture media. Nanoscale 8 (30), 14548–14555. https://doi.org/10.1039/c6nr03246j.

Li, Y., Yuan, H., von dem Bussche, A., Creighton, M., Hurt, R.H., Kane, A.B., Gao, H., 2013. Graphene microsheets enter cells through spontaneous membrane penetration at edge asperities and cornersites. Proc. Natl. Acad. Sci. U. S. A. 110 (30), 12295–12300. https://doi.org/10.1073/pnas.1222276110.

Liao, K.H., Lin, Y.S., Macosko, C.W., Haynes, C.L., 2011. Cytotoxicity of graphene oxide and graphene in human erythrocytes and skin fibroblasts. ACS Appl. Mater. Interfaces 3 (7), 2607–2615. https://doi.org/10.1021/am200428v.

Mondal, S., Thirupathi, R., Rao, L.P., Atreya, H.S., 2016. Unraveling the dynamic nature of protein–graphene oxide interactions. RSC Adv. 6, 52539–52548. https://doi.org/10.1039/C6RA03759C.

OECD, 2010. Test No. 429: Skin Sensitization: Local Lymph Node Assay, OECD Guideline for the Testing of Chemicals Section 4. OECD Publishing, Paris. https://doi.org/10.1787/9789264071100-en.

OECD, 2018. Test No. 442B: Skin Sensitization: Local Lymph Node Assay: BrdU-ELISA or –FCM, OECD Guidelines for the Testing of Chemicals. Section 4. OECD Publishing, Paris. https://doi.org/10.1787/9789264090996-en.

OECD, 2021. Test No. 497: Defined Approaches on Skin Sensitisation, OECD Guidelines for the Testing of Chemicals. Section 4,. OECD Publishing, Paris. https://doi.org/10.1787/b92879a4-en.

OECD, 2022. Test no. 406: Skin sensitisation Guinea pig maximisation test and Buehler test. In: OECD Guidelines for the Testing of Chemicals, Section 4. OECD Publishing, Paris. https://doi.org/10.1787/9789264070660-en.

Park, M.V.D.Z., Bleeker, E.A.J., Brand, W., Cassee, F.R., van Elk, M., Gosens, I., de Jong, W.H., Meesters, J.A.J., Peijnenburg, W.J.G.M., Quik, J.T.K., Vandebriel, R.J., Sips, A.J.A.M., 2017. Considerations for safe innovation: the case of graphene. ACS Nano 11 (10), 9574–9593. https://doi.org/10.1021/acsnano.7b04120.

Paton, K.R., Varrla, E., Backes, C., Smith, R.J., Khan, U., O'Neill, A., Boland, C., Lotya, M., Istrate, O.M., King, P., Higgins, T., Barwich, S., May, P., Puczkarski, P., Ahmed, I., Moebius, M., Pettersson, H., Long, E., Coelho, J., O'Brien, S.E., McGuire, E.K., Sanchez, B.M., Duesberg, G.S., McEvoy, N., Pennycook, T.J., Downing, C., Crossley, A., Nicolosi, V., Coleman, J.N., 2014. Scalable production of large quantities of defect-free few-layer graphene by shear exfoliation in liquids. Nat. Mater. 13 (6), 624–630. https://doi.org/10.1038/nmat3944.

Pelin, M., Fusco, L., León, V., Martín, C., Criado, A., Sosa, S., Vázquez, E., Tubaro, A., Prato, M., 2017. Differential cytotoxic effects of graphene and graphene oxide on skin keratinocytes. Sci. Rep. 7, 40572. https://doi.org/10.1038/srep40572.

Pelin, M., Sosa, S., Prato, M., Tubaro, A., 2018a. Occupational exposure to graphene-based nanomaterials: risk assessment. Nanoscale 10 (34), 15894–15903. https://doi.org/10.1039/c8nr04950e.

Pelin, M., Fusco, L., Martín, C., Sosa, S., Frontiñán-Rubio, J., González-Domínguez, J.M., Durán-Prado, M., Vázquez, E., Prato, M., Tubaro, A., 2018b. Graphene and graphene oxide induce ROS production in human HaCaT skin keratinocytes: the role of

xanthine oxidase and NADH dehydrogenase. Nanoscale 10 (25), 11820–11830. https://doi.org/10.1039/c8nr02933d.

Pelin, M., Lin, H., Gazzi, A., Sosa, S., Ponti, C., Ortega, A., Zurutuza, A., Vázquez, E., Prato, M., Tubaro, A., Bianco, A., 2020. Partial reversibility of the cytotoxic effect induced by graphene-based materials in skin keratinocytes. Nanomaterials (Basel) 10 (8), 1602. https://doi.org/10.3390/nano10081602.

Schneider, K., Schwarz, M., Burkholder, I., Kopp-Schneider, A., Edler, L., Kinsner-Ovaskainen, A., Hartung, T., Hoffmann, S., 2009. ToxRTool, a new tool to assess the reliability of toxicological data. Toxicol. Lett. 189 (2), 138–144. https://doi.org/10.1016/j.toxlet.2009.05.013.

Shin, S.R., Li, Y.C., Jang, H.L., Khoshakhlagh, P., Akbari, M., Nasajpour, A., Zhang, Y.S., Tamayol, A., Khademhosseini, A., 2016. Graphene-based materials for tissue engineering. Adv. Drug Deliv. Rev. 105 (Pt B), 255–274. https://doi.org/10.1016/j.addr.2016.03.007.

Silva, F.A.L.S., Costa-Almeida, R., Timochenco, L., Amaral, S.I., Pinto, S., Gonçalves, I.C., Fernandes, J.R., Magalhães, F.D., Sarmento, B., Pinto, A.M., 2021. Graphene oxide topical administration: skin permeability studies. Materials (Basel) 14 (11), 2810. https://doi.org/10.3390/ma14112810.

Thompson, B.C., Murray, E., Wallace, G.G., 2015. Graphite oxide to graphene. Biomaterials to bionics. Adv. Mater. 27 (46), 7563–7582. https://doi.org/10.1002/adma.201500411.

Wick, P., Louw-Gaume, A.E., Kucki, M., Krug, H.F., Kostarelos, K., Fadeel, B., Dawson, K. A., Salvati, A., Vázquez, E., Ballerini, L., Tretiach, M., Benfenati, F., Flahaut, E., Gauthier, L., Prato, M., Bianco, A., 2014. Classification framework for graphene-based materials. Angew. Chem. Int. Ed. 53 (30), 7714–7718. https://doi.org/10.1002/anie.201403335.

Xia, X.R., Monteiro-Riviere, N.A., Riviere, J.E., 2010. Skin penetration and kinetics of pristine fullerenes (C60) topically exposed in industrial organic solvents. Toxicol. Appl. Pharmacol. 242 (1), 29–37. https://doi.org/10.1016/j. taap.2009.09.011.

Xiaoli, F., Qiyue, C., Weihong, G., Yaqing, Z., Chen, H., Junrong, W., Longquan, S., 2020. Toxicology data of graphene-family nanomaterials: an update. Arch. Toxicol. 94 (6), 1915–1939. https://doi.org/10.1007/s00204-020-02717-2.